Effects of inflow Mach number on oblique detonation initiation with a two-step induction-reaction kinetic model

Pengfei Yang[a,b,c], Honghui Teng[a,b*], Zonglin Jiang[b,c] , Hoi Dick Ng[d]

[a] *Department of Mechanics, School of Aerospace Engineering, Beijing Institute of Technology, Beijing 100081, China*

[b] *State Key Laboratory of High Temperature Gas Dynamics, Institute of Mechanics, Chinese Academy of Sciences, Beijing 100190, China*

[c] *School of Engineering Sciences, University of Chinese Academy of Sciences, Beijing, 100049, China*

[d] *Department of Mechanical, Industrial and Aerospace Engineering, Concordia University, Montreal, QC, H3G 1M8, Canada*

Abstract

Oblique detonations induced by two-dimensional, semi-infinite wedges are simulated by solving numerically the reactive Euler equations with a two-step induction-reaction kinetic model. Previous results obtained with other models have demonstrated that for the low inflow Mach number M_0 regime past a critical value, the wave in the shocked gas changes from an oblique reactive wave front into a secondary oblique detonation wave (ODW). The present numerical results not only confirm the existence of such critical phenomenon, but also indicate that the structural shift is induced by the variation of the main ODW front which becomes sensitive to M_0 near a critical value. Below the critical $M_{0,cr}$, oscillations of the initiation structure are observed and become severe with further decrease of M_0. For low M_0 cases, the non-decaying oscillation of the initiation structure exists after a sufficiently long-time computation, suggesting the quasi-steady balance of initiation wave systems. By varying the heat release rate controlled by k_R, the pre-exponential factor of the second reaction step, the morphology of initiation structures does not vary for M_0 = 10 cases but varies for M_0 = 9 cases, demonstrating that the effects of heat release rate become more prominent when M_0 decreases. The instability parameter χ is introduced to quantify the numerical results. Although χ cannot reveal the detailed mechanism of the structural shift, a linear relation between χ and k_R exists at the critical condition, providing an empirical criterion to predict the structural variation of the initiation structure.

Keywords: oblique detonation, induction-reaction kinetics, initiation length, initiation structure

1. Introduction

The Oblique Detonation Wave (ODW) is a class of high-speed, compressible reacting flow that can be induced by a wedge in an incoming, supersonic combustible mixture. Besides its basic research value being inherent for this class of flow phenomenon [1], the ODW appears to be a viable option for the development of advanced air-breathing, hypersonic propulsion systems such as ODW engines and ram accelerators [2-6].

The ODW phenomenon induced by two-dimensional, semi-infinite wedges has been a

* Corresponding author.
Email address: hhteng@bit.edu.cn (Honghui Teng)

subject of many theoretical, experimental and, lately, numerical investigations. While the basic foundation for steady ODWs such as wave angles and steady structures has been well established [7-10], there are still a number of outstanding fundamental questions, which are linked to the stability of ODWs. Those include the analysis and prediction of the initiation and unsteady structure of ODWs stabilized in hypersonic combustible flow and the susceptibility of the system to instability.

There have been continuous efforts using numerical simulations to address the aforementioned questions and describe the oblique detonation flow phenomena. For instance, Li et al. [11] revealed that the multi-dimensional oblique detonation structure consists of a non-reactive oblique shock, an induction region, a set of deflagration waves, and an oblique detonation surface all united at a multi-wave point. Another type of initiation process is revealed from later numerical investigations in which the oblique shock-to-detonation transition is found to occur smoothly from a curved shock [12, 13]. Parametric studies were also carried out numerically to investigate the dependence of the transition type on various initial conditions and flow parameters such as the incoming flow Mach number, wedge angle and the reactivity of the mixture [14, 15]. In recent studies, high-resolution numerical simulations also demonstrated more complex ODW formation structures near the transition region, particularly when the inflow Mach number decreases. Several kinds of shock systems are observed, with the induction region ended by an internal CJ detonation wave rather than a set of deflagration waves that are found at low inflow Mach number conditions [16-19]. Beside the complex formation structures, the inherent instability of the ODW is also captured using numerical simulation, showing fine scale, unstable evolution of the oblique detonation surface with sets of transverse waves similar to the unstable frontal structure of normal cellular detonations [14, 20-24].

The effect of chemistry is evident in normal cellular detonations. In this regards, studies have shown that chemical kinetic properties of the combustible mixture directly affect the initiation, limits, degree of instability and propagation mechanism of the normal cellular detonation, see Lee [25], Ng & Zhang [26]. For ODW simulations, most of the aforementioned numerical studies employed a single-step reaction kinetics for the chemical description due to its simplicity for achieving high-resolution simulations to resolve the ODW formation structure and subsequent instability on the oblique detonation surface [21-24]. However, there is a concern whether the simulated phenomenon is physical or a numerical artifact of the single-step rate model due to its simple kinetic description where the bulk reactant is simply assumed to transform into the product via a first-order irreversible Arrhenius reaction and will always react to completion releasing the total chemical energy of the mixture [27].

Although a number of numerical studies adapted the complex chemistry model with detailed chemical reaction rates [13, 17, 28, 29], their research objective was on the global ODW behavior such as its wave angles and stabilization without much focus on the details of the ODW formation structure. Furthermore, those studies are computationally expensive and, thus, often limited to a very small computational domain. Although the latter issue can be addressed with the current computational capability for relatively small detailed reaction mechanism such as those for H_2-air oxidation [30, 31], interpretation of the tremendous amount of information that is generated from the computation still remains difficult to come up with any predictive theoretical model.

To avoid the drawback of one-step Arrhenius kinetics and provide a compromise on the detailed reaction mechanism for a given combustible mixture, a two-step reaction kinetic model,

consisting of a thermally neutral induction step followed by a main heat release reaction layer, can be considered. In practice, the chemical kinetics for typical hydrocarbon mixtures behind detonation wave are known to be chain-branching which proceed by a sequence of different types of chemical reaction stages [32]. The one-step irreversible Arrhenius reaction model used in previous studies is over-simplified in the sense that it does not have the flexibility to model the induction zone. Therefore, the two-step kinetic model has been proposed. This not only inherits the simplicity of global kinetics but is detailed enough to retain the features of real combustion governed by chain-branching kinetics. More important, such a model allows the introduction of two length scales, i.e., induction and reaction lengths, which can be varied independently to change the sensitivity of the chemical reaction and also the shape of the reaction zone structure. It is worth noting that recent studies on detonation phenomena have revealed that the dynamics of the detonation structure is strongly governed not only by the global reaction temperature sensitivity but also the length of induction and main heat release layer [33-38].

Motivated by the aforementioned studies, numerical simulations are thus performed using a two-step chemical kinetic model to analyze the initiation structure of oblique detonation waves induced by a wedge. This study focuses on the structure when the inflow Mach number decreases past a critical value, which forms the new structure featured by a secondary ODW. The formation mechanism of this new structure is discussed and the highly transient dynamic initiation process below the critical Mach number is analyzed. The effects of heat release rate on the initiation structure and critical Mach number are investigated to shed light on how the chemical kinetics influences the initiation.

2. Numerical model and methods

A schematic of a typical ODW induced by a two-dimensional, semi-infinite wedge is shown in Fig. 1. The presence of the wedge in a supersonic combustible inflow induces first an oblique shock wave (OSW). For a high inflow Mach number causing a high post-shock temperature behind the OSW, an exothermic chemical reaction begins, leading to the ODW formation. As in previous computations [15, 17, 24, 30, 31], the coordinate is rotated to the direction along the wedge surface and the Cartesian grid in the rectangular domain enclosed by the dashed line in Fig. 1 is aligned with the wedge surface.

Fig. 1. Schematic of a typical oblique detonation wave

Following many previous studies [14-17, 20-23], the reactive Euler equations are used as governing equations for modeling the ODW flow field. To implement the two-step reaction model for chain-branching kinetics, two additional reaction indexes are introduced: one is the induction reaction index ξ, and the other is the heat release index λ. The transport equations of these new variables are:

$$\frac{\partial(\rho\xi)}{\partial t}+\frac{\partial(\rho u\xi)}{\partial x}+\frac{\partial(\rho v\xi)}{\partial y}=H(1-\xi)\rho k_I \exp\left[E_I\left(\frac{1}{T_S}-\frac{1}{T}\right)\right] \tag{1}$$

$$\frac{\partial(\rho\lambda)}{\partial t}+\frac{\partial(\rho u\lambda)}{\partial x}+\frac{\partial(\rho v\lambda)}{\partial y}=[1-H(1-\xi)]\rho(1-\lambda)k_R \exp\left[-\frac{E_R}{T}\right] \tag{2}$$

with the Heaviside step function

$$H(1-\xi)=\begin{cases}1, & \text{if } \xi \le 1\\ 0, & \text{if } \xi > 1\end{cases} \tag{3}$$

The specific total energy is thus expressed as:

$$e=\frac{p}{\rho(\gamma-1)}+\frac{1}{2}(u^2+v^2)-\lambda Q \tag{4}$$

The variables ρ, u, v, p, e and Q are the density, x- direction velocity, y- direction velocity, pressure, specific total energy, and the amount of chemical heat release, respectively. All the variables have been non-dimensionlized by reference to the uniform unburned state as follows:

$$\rho=\frac{\tilde{\rho}}{\rho_0},\qquad p=\frac{\tilde{p}}{p_0},\qquad T=\frac{\tilde{T}}{T_0},\qquad u=\frac{\tilde{u}}{\sqrt{RT_0}} \tag{5}$$

The dispersion controlled dissipation (DCD) scheme [39] together with a 3rd order Runge-Kutta algorithm are used to approximate numerically the solution of the governing equations. The DCD scheme is designed to adjust the dispersion around the strong discontinuity and thus, non-physical oscillations near the shock wave are suppressed. Generally, it is one kind of total variation diminishing (TVD) schemes, which can achieve 2nd order accuracy in the smooth flow field. The main parameters are set to be Q = 50, γ = 1.2, E_I = 5.0 T_s, E_R = 1.0 T_s, where T_s is the post-shock temperature. For reference, the corresponding parameters of the CJ detonation are shown in Table 1, in which the Mach number is that in the shock-fixed frame.

Table 1 Parameters of the CJ detonation based on chosen reaction parameters

	VN point	CJ points
Pressure	42.063	21.533
Temperature	4.813	11.998
Mach number	0.324	1.000

To complete the model, two kinetic parameters, k_I and k_R, are necessary. In this study, k_I = -u_{vn} where u_{vn} is the particle velocity behind the shock front in the shock-fixed frame for the corresponding Chapman-Jouguet (CJ) detonation, whereby the induction length of the CJ detonation is fixed to unity, i.e., Δ_I = 1.0. The bifurcation parameter k_R, whose default value is 1.0, controls the heat release rate and is employed here to vary the heat release process. This process is characterized by the reaction length scale Δ_R, and the instability parameter χ introduced in [35,38] is employed to analyze the numerical results. Details on how to calculate Δ_R and χ are given in Appendix A. To simulate one specific combustible gas mixture, the model parameters can be adjusted to fit the results from detailed chemistry models.

For the CJ detonation based on the given chemical model parameters, χ is about 0.832. It is worth noting that for purely a one-dimensional (1D) configuration [25, 35], the 1D detonation wave becomes unstable (with longitudinal pulsations) when χ is higher than 1.2 to 1.6. Using this one-dimensional stability boundary as a way to assess the degree of cellular instability, it is found that close to or below this critical χ the cellular detonation front pattern is typically very regular. However, it is well established that multidimensional detonations are more susceptible to instability and for typical conditions, the multidimensional detonation is inherently unstable forming the cellular structure [40]. Moreover, the growth rates and manifestation can vary significantly, particularly for ODW where the overdriven effect can inhibit unstable modes with fast growth rate and damp the development of the cellular unstable surface [41]. Thus, the χ value of 0.832 based on the given chemical model parameters, especially k_R = 1.0, indicates that the present study focuses on weakly unstable detonations. Effects of k_R, whose default value is 1.0,

will be studied in Sect. 3.4.

In this study, the wedge angle θ is fixed to be 30° in all cases, and the inflow Mach number M_0, is the bifurcation parameter varying mainly below 10. Unless specified, the length of the computational domain is fixed to be 150, with the wedge starting from x = 5; and the width varies case by case. Initially the whole flow field has uniform density, velocity and pressure: both the density and pressure are unity as the unburned state, and the velocity is calculated and projected according to M_0 and θ as shown in Fig. 1. The left and upper boundaries are modelled as inflow boundary conditions, where the parameters are fixed to be constant due to the supersonic flow. Outflow conditions extrapolated from the interior are implemented on the right and lower boundaries before the wedge. Slip boundary condition is used on the wedge surface, which starts from x = 5 on the lower boundary. All the cases of this study try to get the steady ODW by carrying out a sufficiently long-time computation. Except for special cases with low M_0 shown later on in Figs. 8-10, most results are found to be steady after the initial transient evolution and do not evolve with time. The unsteady flow features, occurring at the low inflow Mach number regime, will be illustrated in Fig. 9 and discussed in section 3.3.

3. Numerical results and discussion

3.1 Basic structure and resolution study

A test case is first simulated to illustrate the basic structure and verify the effect of numerical grid resolution. Results with wedge angle θ = 30° and incident Mach number M_0 = 10 are shown in Fig. 2. The wedge starts from x = 5, from where the oblique shock is initiated. The upper half shows the results obtained using the grid scale of 0.050, while the lower half shows those from the grid scale of 0.025. These resolutions correspond 20 and 40 grids per the induction length of the CJ detonation, respectively. It can be observed that the oblique shock-to-detonation transition forms around x = 40 to 80 in both results, whose difference is hardly visible. The region beneath the oblique shock can be viewed as the induction zone, which is terminated by the main heat release after x = 40. In fact, a significant number of grid points has covered this enlarged induction region. Generally, the grid scale 0.050 is enough to capture the ODW structure and, thus, is used subsequently.

Fig. 2. Density field of the oblique detonation with M_0 = 10, grid scale 0.050 (upper) and 0.025 (lower)

Fig. 3. Pressure (black) and temperature (red) along the wedge with M_0 = 10, y = 0 (a) and y = 5 (b), grid scale 0.050 (solid) and 0.025 (dashed)

The shock-to-detonation transition shown in Fig 2 corresponds to the smooth transition by a curved shock [12, 13]. To analyze its characteristics and further verify the resolution, the pressure and temperature along two lines paralleled with the x- axis, at y = 0 and y = 5, are shown in Fig. 3. The parameters along the wedge, i.e., y = 0, are plotted in Fig. 3a, while the parameters along the line y = 5 are plotted in Fig. 3b to examine the transition region. Here the solid lines show the results from the grid scale of 0.050 and the dashed lines show those from the grid scale of 0.025. The solid and dashed curves are seen to almost overlap one another and the difference is found to be negligible. For the purpose of this work, the chosen grid size provides converged, global,

initiation structures, sufficient to guarantee the reliability of the conclusion. Nevertheless, a higher resolution is certainly desirable to resolve the small-scale details within the wave structure.

These numerical results show two different shock-reaction relations. In Fig. 3a, the post-shock temperature is low so there is a long induction length, and then the modest increase of pressure and temperature can be observed downstream. In Fig. 3b, the post-temperature is high, but not enough to establish the overdriven detonation like the fully-developed oblique detonation surface, so the pressure rises and generates a peak downstream, suggesting a weak coupling between the oblique shock and heat release. These phenomena are similar to those in our previous study, in which the detailed analysis on the initiation mechanism can be found [30].

3.2 The dependence of initiation structures on inflow Mach number

Fig. 4. Temperature fields of oblique detonations with M_0 = 11 (a), 10 (b), and 9 (c)

ODW initiation structures at different M_0 are shown in Fig. 4. It can be observed that the oblique shock-to-detonation transition moves upstream for increasing M_0, illustrating that the oblique detonation onset is easier to trigger. This is physically reasonable because of the high post-shock temperature resulted from the strong oblique shock. Furthermore, it can be observed that the transition type of oblique shock-to-detonation changes in Fig. 4, i.e., from an abrupt transition to a smooth one by a curved shock. This is not surprising considering the initiation structure dependence on M_0 has also been illustrated before, either using a one-step Arrhenius chemical kinetic model [15] or a detailed chemical reaction model [42], and similar results are observed.

For a quantitative analysis, the length of the initiation region and the oblique detonation angle are determined. A parametric study is performed to investigate the dependence of the length L_w and oblique detonation angle β on the inflow Mach number M_0 where L_w is defined from the wedge tip to the starting point of main heat release along the x-axis at y = 0, while β is measured on the detonation surface excluding the initiation region with curved shock. As shown in Fig. 5, both L_w and β decrease monotonically with increasing M_0. The variation of β with respect to different M_0 as determined in the present simulations is found to be consistent with the Rankine–Hugoniot analysis given in Appendix B.

Fig. 5. Variation of L_w and β as a function of M_0

Fig. 6. Temperature fields (black lines denote the sonic location) of oblique detonations with (a) M_0 = 8.9 and (b) M_0 = 8.8

The monotonic function between L_w and M_0 does not exist when M_0 decreases past a certain critical value, $M_{0,cr}$, due to the formation of different flow structures. The temperature fields around the initiation region for M_0 = 8.9 and 8.8 are shown in Fig. 6. Clearly the structure of M_0 = 8.9 is similar to those shown above, but the structure of M_0 = 8.8 has a different wave configuration. Besides the main ODW surface, a secondary ODW forms at the end of the shocked gas, extending downstream with a regular reflection on the wedge. Furthermore, the sonic location takes more areas in the combustion product. The formation of secondary ODW has been

confirmed, while the Mach reflection on the wedge is observed [17, 19]. Nevertheless, the relation between these two structures is not yet clear. Comparing the flow fields, the heat release starting position on the wedge moves downstream when M_0 decreases, illustrating similar trend of L_w as shown in Fig. 4 and 5. Hence, the structural shift should be attributed to the upstream jump of the main ODW position, which becomes very sensitive to M_0 at the critical condition.

Fig. 7. Sketches of the three types of wave structures

From the above results, there are three types of wave structures dependent on M_0, and these are sketched in Fig. 7. The first structure appears in the cases of relatively higher M_0, featured by a curved shock connecting OSW, ODW, reaction front, and slip line. It induces the smooth transition and beneath the curved shock in the transition region, the reaction front appears so the shocked gas behind OSW combusts. Decreasing M_0 generates the second structure featured by an abrupt transition through one multi-waves point, as shown in Fig. 7b. In this structure, the curved shock evolves into a multi-wave point, beneath which the reaction front appears like the last structure. With further decrease of M_0, the shock-induced reactive wave front becomes the secondary ODW, indicated by ODW2 in Fig. 7c. The two transition Mach numbers corresponding the structure shift are 9.2 and 8.8 in this study. It is also found that the last structure is unstable and its long-period behaviors are studied in the later part of this work. Theoretically, there is a minimal M_0 below which the shock becomes detached. Based on the given wedge angle and chemical model parameters, this M_0 is determined to be 7.87.

3.3 Discussion on the low inflow Mach number effects

Fig. 8. Variation of initiation lengths as function of M_0

Although previous studies have demonstrated that the structure near the initiation region becomes increasingly complex when M_0 decreases [16-19], this phenomenon still lacks detailed study. Except the existence of the critical M_0 corresponding to the structure shift, how the structure evolves after the shift and what controls the shift are still not well understood. To describe more clearly these observations, another length L_{det} to characterize the ODW surface needs to be introduced. Here, L_{det} is defined along the line parallel to the x- axis, starting from the wedge tip and ending by the multi-waves point, i.e., the front tip of the ODW, as shown in Fig. 6. More cases are simulated and the variation of L_{det} and L_w as a function of M_0 is shown in Fig. 8. It is observed that both characteristic lengths increase when M_0 decreases from a large number until $M_{0,cr}$ = 8.9, as shown in the right part of Fig. 8. Afterward, an abrupt change of L_{det} appears first when M_0 decreases from 8.9 to 8.8. The change of L_{det} induces the change of L_w, displaying similar but a smoother trend although the maximum L_w length appears at the lower M_0 = 8.7.

Fig. 9. Evolution of the heat release starting position on the wedge with M_0 = 8.6-8.3

Investigation of the flow features after the structure shift is scarce in the literature, partly because the structure featured by the secondary ODW needs a longer relaxation period for the flow field to self-adjust. Benefiting from the advantage of this model, we aim to carry out a sufficiently long-time calculation to achieve the steady structure. In the case of M_0 = 8.7, the

structure is similar to that of M_0 = 8.8 shown in Fig. 6, but decreasing M_0 further induces a more transient process. The temporal evolution of the heat release starting point on the wedge, i.e., L_w plus the pre-wedge length 5.0, is given in Fig. 9. Because the simulation starts with a uniform flow field, an oblique shock first forms and subsequently induces the ODW initiation. Initially the ODW angle increases and L_w remains the same, as shown by the plateau before about t = 200 in Fig. 9. However, after the ODW angle increases over a certain value, the surface propagates upstream and generates the new structure featured by the secondary ODW. In the case of M_0 = 8.6, L_w is found to converge after the initial oscillation following a long-time decay. The transient fluctuations become significant when M_0 decreases further. L_w is found to fluctuate around an equilibrium position, and the oscillation amplitude becomes large with lower M_0. It should be mentioned that L_{det} also shows the similar fluctuation behaviors, with larger amplitude. The successful initiation of ODW above M_0 = 8.9 usually takes the time below t < 300, but the oscillation of the cases for $M_0 \leq 8.5$ would not decay even after t = 2500. Therefore, this non-decaying oscillation appears not artificial but reflects the inherent characteristics of the ODW. Previous studies [17-19] have found that the transient processes may occur in the low M_0 cases, but the non-decaying oscillation has never been pointed out to our knowledge. Generally, these phenomena reflect the quasi-steady balance of the OSW, the main ODW, and the secondary ODW. For engineering applications, this is crucial in the design of ODW engines as it is the foundation to determine the lower flight Mach number limit of ODW-based propulsion systems. Because the detonation is only weakly unstable, with the instability parameter χ about 0.832, the cellular structures are not observed in the ODW surface within the present computational domain.

Fig. 10. Theoretical and numerical instability parameter χ as function of M_0

Since the unsteady flow appears soon after the structural shift, the criterion on the structural shift may perhaps be related with the inherent detonation instability. To examine the connection, theoretical and numerical instability parameter χ values are shown in Fig. 10, whose calculation processes are given in Appendix A. Obviously, the numerical χ based on the simulation results is sensitive to M_0, but the theoretical χ based on the oblique shock/detonation relation is not. The theoretical value is always higher than the corresponding numerical one, demonstrating the curved oblique detonation angle effects. On the theoretical χ curve, the variation is very shallow because when M_0 decreases, oblique detonation angle increases, and finally these two parameters have the opposite effects on χ. Moreover, on the numerical χ curve, there is a jump between M_0 = 9.2 and 9.3. This jump is indeed found to correspond to the change of transition type where the oblique shock-detonation transition changes from a smooth curved shock to an abrupt one with a multi-wave point (see Fig .4). However, near $M_{0,cr}$ = 8.9, χ is about 0.79 and increases slightly. In both the theoretical and numerical χ curves, no inflection point can be observed. Thus, the instability parameter χ alone unfortunately cannot explain directly the structural shift with the appearance of a secondary ODW.

3.4 Effects of heat release rate

Fig. 11. Temperature field of oblique detonations with M_0 = 10, k_R = 0.5 (a), 1.0 (b), and 1.5 (c)

Fig. 12. Temperature field of oblique detonations with $M_0 = 9$, $k_R = 0.5$ (a), 1.0 (b), and 1.5 (c)

By varying the heat release rate controlled by the pre-exponential factor of the second reaction step, the effects of chemical kinetics on the initiation structure are also investigated. As the main advantage of this two-step induction-reaction kinetic model, it is convenient to change the heat release rate to study its effects on the initiation structure. This rate controls the detonation instability by changing the coupling between the shock and heat release [35], and plays a vital role in the detonation initiation. The consequence of varying k_R while keeping other chemical parameters constant is the change of the induction-to-reaction length ratio, which is known to affect gaseous detonation hydrodynamic stability [26, 34, 36]. Figure 11 shows the effects of k_R on the ODW initiation structure for $M_0 = 10$. Compared with the aforementioned results with $k_R = 1.0$, the general wave configuration appears the same but the post-shock temperature contours change obviously. It is observed that L_w is independent of k_R, while L_{det} increases when k_R decreases, and vice versa. It is worth noting that L_w denotes primarily the ignition process and thus is not influenced by the heat release rate. In contrast, L_{det} can be affected by both the ignition and heat release processes and the effect of k_R on this length scale becomes apparent. The effects of k_R with $M_0 = 9$ in Fig. 12 show similar variation trend. The main difference of these two cases is that the initiation structure varies from the abrupt transition to the smooth transition in Fig. 12, demonstrating that the effects of heat release rate becomes more prominent when M_0 decreases. Although cellular structures on the ODW surface are not observed in this study within the chosen computational domain, our recent study [43] demonstrates that the formation of triple points on the ODW surfaces is more promptly when k_R increases further above 1.5.

Fig. 13. Variation of the critical Mach number $M_{o,cr}$ as a function of k_R

Because the heat release rate may change the structure of oblique detonations, it is deduced that the structural shift should be influenced by k_R. As introduced in Sec.2, k_R controls the heat release rate, and then determines the induction-to-reaction length ratio. Thus, it may be viewed as a parameter on the gas property, and k_R-$M_{o,cr}$ relation reveals the connection between two key gas-dynamic and chemical dynamic parameters used in this structural shift study. To investigate the effects of heat release rate on the critical Mach number, Fig. 13 shows the variation of critical $M_{0,cr}$ as a function of k_R. It can be seen that $M_{0,cr}$ remains at a value of 8.9 with k_R above 1.0, but decreases monotonically to as low as 8.6 when k_R is reducing from 1.0 to 0.5. Because the critical M_0 corresponds to the structure shift induced by the low inflow Mach number, this variation demonstrates the complexity of the heat release rate at the critical condition. However, the variation of $M_{0,cr}$ is limited in a narrow regime, i.e. 8.6 - 8.9, and further increasing k_R would not change $M_{0,cr}$ when k_R above 1.0. It is observed that the initiation structures in the case of $k_R = 1.0$ and 1.5, shown in Fig. 11, have obvious differences, but the corresponding values of $M_{o,cr}$ remain the same. In short, although the initiation structure is sensitive to the heat release rate, the structural shift is not, suggesting different features in two phenomena.

Fig. 14. Variation of the instability parameter χ_{cr} as a function of k_R

To elucidate the mechanism of the structural shift, the instability parameter χ at the critical condition is studied. Although χ cannot predict the structural shift independently as discussed in section 3.3, it is found that a linear relation can be obtained between χ_{cr} and k_R, as illustrated in Fig. 14. This relation is expressed as:

$$\chi_{cr} \approx 0.760\, k_R + 0.036 \tag{6}$$

This linear function demonstrates that the combination of χ and k_R can provide an empirical criterion to predict the structural shift, although the constants in Eq. 6 need to be analyzed and elaborated further. Previous studies, e.g., [35], demonstrates that the instability parameter χ is a good criterion to predict the instability (or more specifically, the cellular regularity) of CJ detonations. For both 1D and 2D cases, the detonations become unstable when χ increases. The mechanism can be described by the sensitivity to temperature fluctuations of the characteristic induction length relative to the characteristic exothermic reaction length. Nevertheless, the ODW of this study is not CJ but overdriven detonation, and the structural shift is also different from the longitude or transverse instability studied before. However, χ together with k_R can predict the structural shift, demonstrating χ is not limited into the classic detonation instability studies, but also useful to investigate the ODW phenomena associated with the low inflow Mach number. It should be mentioned that χ_{cr} is different slight from χ in normal detonations because the ratio of induction and heat release lengths vary along the detonation. χ_{cr} is a deduced parameter from gas-property parameter χ, but it only reflects the local length ratio related with the structural shift. The underlying mechanism is that the structural shift is also dominated by the characteristic combustion lengths, and the inherent relations between these kinds of phenomena deserve more attention in the future.

4. Concluding remarks

Oblique detonations induced by two-dimensional, semi-infinite wedges are simulated by solving the Euler equations with a two-step reaction model for chain-branching kinetics. Consistent with previous studies, the present numerical results also show that initiation can be triggered by either an abrupt or a smooth transition with a curved shock, and the transition type depends on the inflow Mach number M_0. By decreasing M_0 gradually, it is found that there exists a critical $M_{0,cr}$ value below which the wave in the shocked gas changes into a secondary ODW, accompanying an abrupt shift of the main ODW position. Therefore, there exists three topologies of wave structures totally, and this study focuses the one featured by a secondary ODW. In this topology, the structural shift is found to be dominated by the main ODW, whose position is sensitive near the critical $M_{0,cr}$. By defining the variation of initiation lengths L_w and L_{det}, the reverse variation trend of the initiation lengths with M_0 is analyzed and discussed.

Benefiting from the simplicity of the chemical model but yet capable of capturing characteristics of chain-branching reaction kinetics, the ODW structure evolution below the critical $M_{0,cr}$ is studied, which requires a long computational time for the flow to self-adjust. It is found that ODW initiation structures are indeed shown to be transient, oscillating around an equilibrium position. Such non-decaying oscillation of the initiation structure is observed for the first time. Using the two-step chain-branching chemical kinetics, the two reaction length scales, namely, the induction and main heat release layer can be varied independently. This study investigates the effects of the chemical kinetics by varying the heat release rate controlled by the pre-exponential factor of the second reaction step. It is observed that the morphology of initiation structures varies for M_0 = 9 cases, demonstrating the effects of heat release rate becomes more prominent when M_0 decreases. However, the structural shift is not sensitive to the heat release rate, so the critical M_0 varies in a narrow regime.

To elucidate the effects of inflow Mach number, especially the structure shift observed when M_0 decreases, quantitative analysis is performed by examining the instability parameter χ. Near the initiation region, a large, curved oblique detonation angle appears, so both the theoretical and numerical χ curves are calculated. Nevertheless, the inflection point cannot be observed in both curves at the critical condition, demonstrating the instability parameter χ cannot explain the structural shift independently. However, a linear relation between χ and k_R exists at the critical condition, providing an empirical criterion to predict the structural shift.

Acknowledgement

This research is supported by The National Natural Science Foundation of China NSFC Nos. 91641130, 11372333 and 51376165; and H.D. Ng acknowledges the support by The Natural Sciences and Engineering Research Council of Canada (NSERC).

Appendix A

The instability parameter χ used in this study is calculated by:

$$\chi = \frac{E_I}{T_S}\frac{\Delta_I}{\Delta_R} \tag{a1}$$

where Δ_I and Δ_R denote the characteristic induction length and reaction length, respectively [35]. Δ_I is defined by the induction reaction index ξ, and Δ_R is defined by the ratio of the particle velocity at the end of heat release zone in shock-fixed coordinates to the maximum thermicity, which is

$$\Delta_R = \frac{u_{CJ}}{\dot{\sigma}_{max}} \tag{a2}$$

and the thermicity is expressed as

$$\dot{\sigma} = (\gamma - 1)\frac{Q}{c^2}\frac{d\lambda}{dt} \tag{a3}$$

For CJ detonations based on the given chemical model parameters, χ is about 0.832 with the default k_R 1.0. Table a1 lists the reaction zone lengths and instability parameters dependent on k_R, demonstrating that the reaction zone length becomes short by increasing k_R. With k_R equal to 0.5 and 1.5, χ becomes 0.418 and 1.243, respectively.

Table a1 Reaction zone lengths and instability parameters of CJ detonations

k_R	Δ_R	χ
0.5	11.965	0.418
0.6	9.979	0.501
0.7	8.561	0.584
0.8	7.497	0.667
0.9	6.669	0.750
1.0	6.007	0.832
1.1	5.466	0.915

1.2	5.014	0.997
1.3	4.632	1.079
1.4	4.305	1.161
1.5	4.021	1.243

For oblique detonations, two evaluations of the instability parameter, namely the theoretical one and the numerical one, are used in this study. As oblique detonations are two-dimensional, the way of how to determine Δ_I and Δ_R is critical. Referring to the definition of detonation overdriven degree, the characteristic lengths are chosen to be along the direction perpendicular to wave surfaces. For the theoretical χ, the oblique detonation angle β is first calculated analytically from oblique shock/detonation relations. Then the overdriven degree of ODW surface is calculated, and used in the 1D overdriven detonation simulation to get the corresponding length scales. Because the theoretical oblique detonation angle is calculated here by assuming the instant heat release across the ODW surface, hence the theoretical χ only represents the instability of far field ODWs.

For the numerical χ, the oblique detonation surface varies near the initiation region, illustrating an initially steep, curved oblique angle. In this study, in order to calculate the numerical χ, we use the largest angle located on the tip of the ODW surface. The angle β is calculated by two adjacent points along the constant pressure or temperature contours on the detonation surface near the tip. Based on the (x, y) positions of the points, the oblique detonation angle β is calculated, and then the other procedure to find χ is similar to that used for the theoretical one. Because the angle of the tip is the largest, the numerical χ is thus the smallest one. On the other side, the steep angle near the initiation region relaxes to the theoretical angle, so the theoretical χ is the largest one.

Appendix B

Fig. b1. Detonation polar curves in the case of M_0 = 9 and 11

Following the fluid conservation laws, the oblique shock wave angle β_s is determined by the wedge angle θ and the incident Mach number M_0 :

$$\frac{\tan\beta_s}{\tan(\beta_s-\theta)}=\frac{(\gamma+1)M_0^2\sin^2\beta_s}{(\gamma-1)M_0^2\sin^2\beta_s+2} \qquad (b1)$$

The oblique detonation wave angle β can be calculated by

$$\frac{\tan\beta}{\tan(\beta-\theta)}=\frac{(\gamma+1)M_0^2\sin^2\beta}{\gamma M_0^2\sin^2\beta+1-\sqrt{(M_0^2\sin^2\beta-1)^2-2Q(\gamma-1/\gamma)M_0^2\sin^2\beta}} \qquad (b2)$$

The variables have been referred in the text. By setting Q = 0, Eq. b2 becomes Eq. b1, demonstrating the two equations are consistent. Solving the above equations, β-θ relation can be plotted as the detonation/shock polar. The detonation polar curves based on the paramters of this study, i.e. Q = 50, γ = 1.2, and M_0 = 9 and 11, are shown in Fig b1. It is demonstrated that the high M_0 induces the small β in the case of same θ.

Fig. b2. Theoretical and numerical β as a function of M_0

The theoretical M_0-β relation in the case of θ = 30° is shown in Fig. b2, and compared with the numerical results shown in Fig. 5. It is observed that the curves are close to each other and show similar trends. The difference becomes significant when M_0 decreasing, which is reasonable considering the complicated phenomena induced by the low M_0 discussed in this study.

Reference

[1] J.M. Powers, Oblique detonations: Theory and propulsion applications, in: J. Buckmaster, T.L. Jackson, and A. Kumar (Eds.) , Combustion in High Speed Flows, Springer Netherlands, 1994, pp. 345-371.

[2] G. P. Menes, H. G. Adelman, J. L. Cambier, J. V. Bowles, Wave combustors for trans-atmospheric vehicles, J. Propul. Power 8 (1992) 709-713.

[3] G. D. Roy, S. M. Frolov, A. A. Borisov, D. W. Netzer, Pulse detonation propulsion: challenges, current status, and future perspective, Prog. Energy Combust. Sci. 30 (2004) 545-672.

[4] F. K. Lu, Prospects for detonations in propulsion, 9th International Symposium on Experimental and Computational Aerothermodynamics of Internal Flows (2009), Paper No. IL-2.

[5] P. Wolanski, Detonation propulsion, Proc. Combust. Inst. 34 (2013) 125-158.

[6] M. A. Nettleton, The applications of unsteady, multi-dimensional studies of detonation waves to ram accelerators, Shock Waves 10 (2000) 9-22.

[7] R. A. Gross, Oblique detonation waves, AIAA J. 1 (1963) 1225-1227.

[8] D. T. Pratt, J. W. Humphrey, D. E. Glenn, Morphology of standing oblique detonation waves, J. Propul. Power 7 (1991) 837-845.

[9] S. A. Ashford, G. Emanuel, Wave angle for oblique detonation waves, Shock Waves 3 (1994) 327-329.

[10] G. Emanuel, D. G. Tuckness, Steady, oblique, detonation waves, Shock Waves 13 (2004) 445-451.

[11] C. Li, K. Kailasanath, E. S. Oran, Detonation structures behind oblique shocks, Phys. Fluids 6 (1994) 1600-1611.

[12] V. V. Vlasenko, V. A. Sabel'nikov, Numerical simulation of inviscid flows with hydrogen combustion behind shock waves and in detonation waves, Combust. Explos. Shock Waves 31 (1995) 376-389.

[13] L. da Silva Figueira, B. Deshaies, Stabilization of an oblique detonation wave by a wedge: a parametric numerical study, Combust. Flame 121 (2000) 152-166.

[14] M. V. Papalexandris, Numerical study of wedge-induced detonations. Combust. Flame 120 (2000) 526-538.

[15] H. H. Teng, Z. L. Jiang, On the transition pattern of the oblique detonation structure, J. Fluid Mech. 713 (2012) 659-669.

[16] J. Y. Choi, E. J. Shin, I. S. Jeung, Unstable combustion induced by oblique shock waves at the non-attaching condition of the oblique detonation wave, Proc. Combust. Inst. 32 (2009) 2387-2396.

[17] H. Teng, Y. Zhang, Z. Jiang. Numerical investigation on the induction zone structure of the oblique detonation waves. Computers & Fluids 95 (2014) 127-131.

[18] Y. Liu, D. Wu, S. B. Yao, J. P. Wang, Analytical and numerical investigations of

wedge-induced oblique detonation waves at low inflow Mach number, Combust. Sci. Technol. 187 (2015) 843-856.

[19] Y. Liu, Y. S. Liu, D. Wu, J. P. Wang, Structure of an oblique detonation wave induced by a wedge, Shock Waves 26 (2016) 161-168.

[20] M. J. Grismer, J. M. Powers, Numerical predictions of oblique detonation stability boundaries, Shock Waves 6 (1996) 147-156.

[21] J. Y. Choi, D. W. Kim, I. S. Jeung, F. Ma, V. Yang, Cell-like structure of unstable oblique detonation wave from high-resolution numerical simulation, Proc. Combust. Inst. 31 (2007) 2473-2480.

[22] M. Y. Gui, B. C. Fan, G. Dong, Periodic oscillation and fine structure of wedge induced oblique detonation waves, Acta Mech. Sin. 27 (2011) 922-928.

[23] J. Verreault, A. J. Higgins, R. A. Stowe, Formation of transverse waves in oblique detonations, Proc. Combust. Inst. 34 (2013) 1913-1920.

[24] P. Yang, H. D. Ng, H. Teng, Z. Jiang. Initiation structure of oblique detonation waves behind conical shocks. Phys. Fluids 29 (2017) 086104

[25] J. H. S. Lee, The Detonation Phenomenon, Cambridge University Press, New York, 2008.

[26] H. D. Ng, F. Zhang, Detonation instability, in: F. Zhang (Eds.), Shock Wave Science and Technology Reference Library, Vol. 6, Springer Berlin Heidelberg , 2012, pp. 107-212.

[27] H. D. Ng, J. H. S. Lee, Direct initiation of detonation with a multi-step reaction scheme, J. Fluid Mech. 476 (2003) 179-211.

[28] J. L. Cambier, H. Adelman, G. P. Menees, Numerical simulations of an oblique detonation wave engine, J. Prop. 6 (1990) 315-323.

[29] G. Fusina, J. P. Sislian, B. Parent, Formation and stability of near Chapman-Jouguet standing oblique detonation waves, AIAA J. 43 (2005) 1591-1604.

[30] T. Wang, Y. N. Zhang, H. H. Teng, Z. L. Jiang, H. D. Ng, Numerical study of oblique detonation wave initiation in a stoichiometric H_2-air mixture, Phys. Fluids 27 (2015) 096101.

[31] Y. N. Zhang, J. S. Gong, T. Wang, Numerical study on initiation of oblique detonations in H2-air mixtures with various equivalence ratios, Aerosp. Sci. Technol. 49 (2016) 130-134.

[32] K. K. Kuo, Principles of Combustion, 2nd edition, Wiley-Interscience, New York, 2005.

[33] M. Short, J. J. Quirk, On the nonlinear stability and detonability limit of a detonation wave for amodel three-step chain-branching reaction, J. Fluid Mech. 339 (1997) 89-119.

[34] M. Short, G. J. Sharpe, Pulsating instability of detonations with a two-step chain-branching reaction model: theory and numerics, Combust. Theory Model. 7 (2003) 401-416.

[35] H. D. Ng, M. I. Radulescu, A. J. Higgins, N. Nikiforakis, J. H. S. Lee, Numerical investigation of the instability for one-dimensional Chapman-Jouguet detonations with chain-branching kinetics, Combust. Theory Model. 9(3) (2005) 385-401.

[36] M. I. Radulescu, H. D. Ng, J. H. S. Lee, B. Varatharajan, The effect of argon dilution on the stability of acetylene-oxygen detonations, Proc. Combust. Inst. 29 (2002) 2825-2831.

[37] C. Leung, M. I. Radulescu, G. J. Sharpe, Characteristics analysis of the one-dimensional pulsating dynamics of chain-branching detonations, Phys. Fluids 22(12) (2010) 126101.

[38] J. Tang, M. I . Radulescu, Dynamics of shock induced ignition in Fickett's model: Influence of χ, Proc. Combust. Inst. 34(2) (2013) 2035-2041

[39] Z. L. Jiang, On dispersion-controlled principles for non-oscillatory shock-capturing schemes, Acta Mech. Sin. 20(1) (2004) 1-15.

[40] M. Short, D.S. Stewart, Cellular detonation instability. Part 1. A normal-mode linear analysis. J. Fluid Mech. 368 (1998) 229–262.

[41] H. H. Teng, Z. L. Jiang, H. D. Ng, Numerical study on unstable surfaces of oblique detonations, J. Fluid Mech. 744 (2014) 111-128.

[42] H. H. Teng, H. D. Ng, Z. L Jiang, Initiation characteristics of wedge-induced oblique detonation waves in a stoichiometric hydrogen-air mixture, Proc. Combust. Inst. 36 (2017) 2735-2742.

[43] P. Yang, H. Teng, H. D. Ng, Z. Jiang, A numerical study on the instability of oblique detonation waves with a two-step induction-reaction kinetic model, submitted to Proc. Combust. Inst.

Figure 1
Click here to download high resolution image

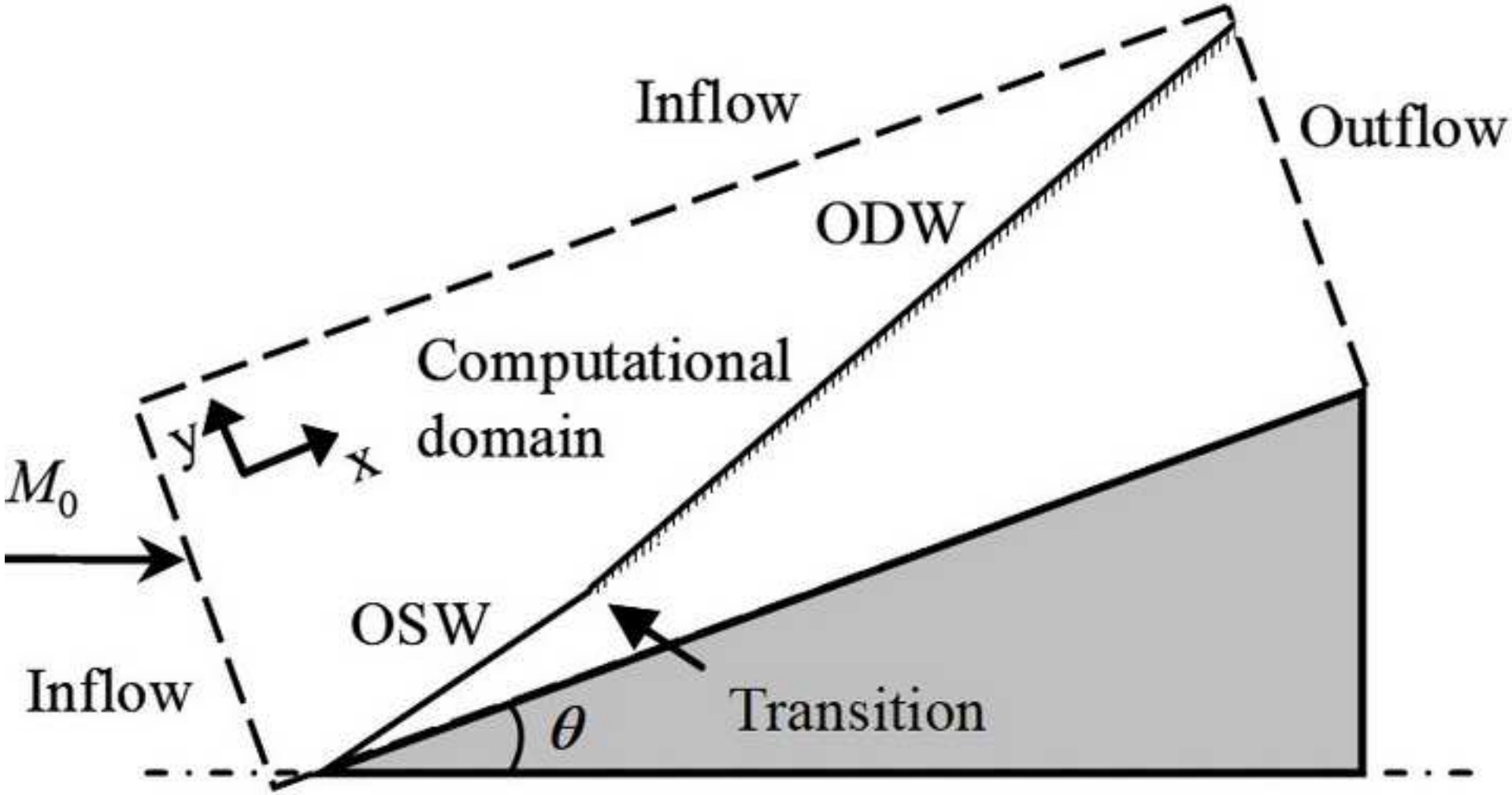

Figure 2
Click here to download high resolution image

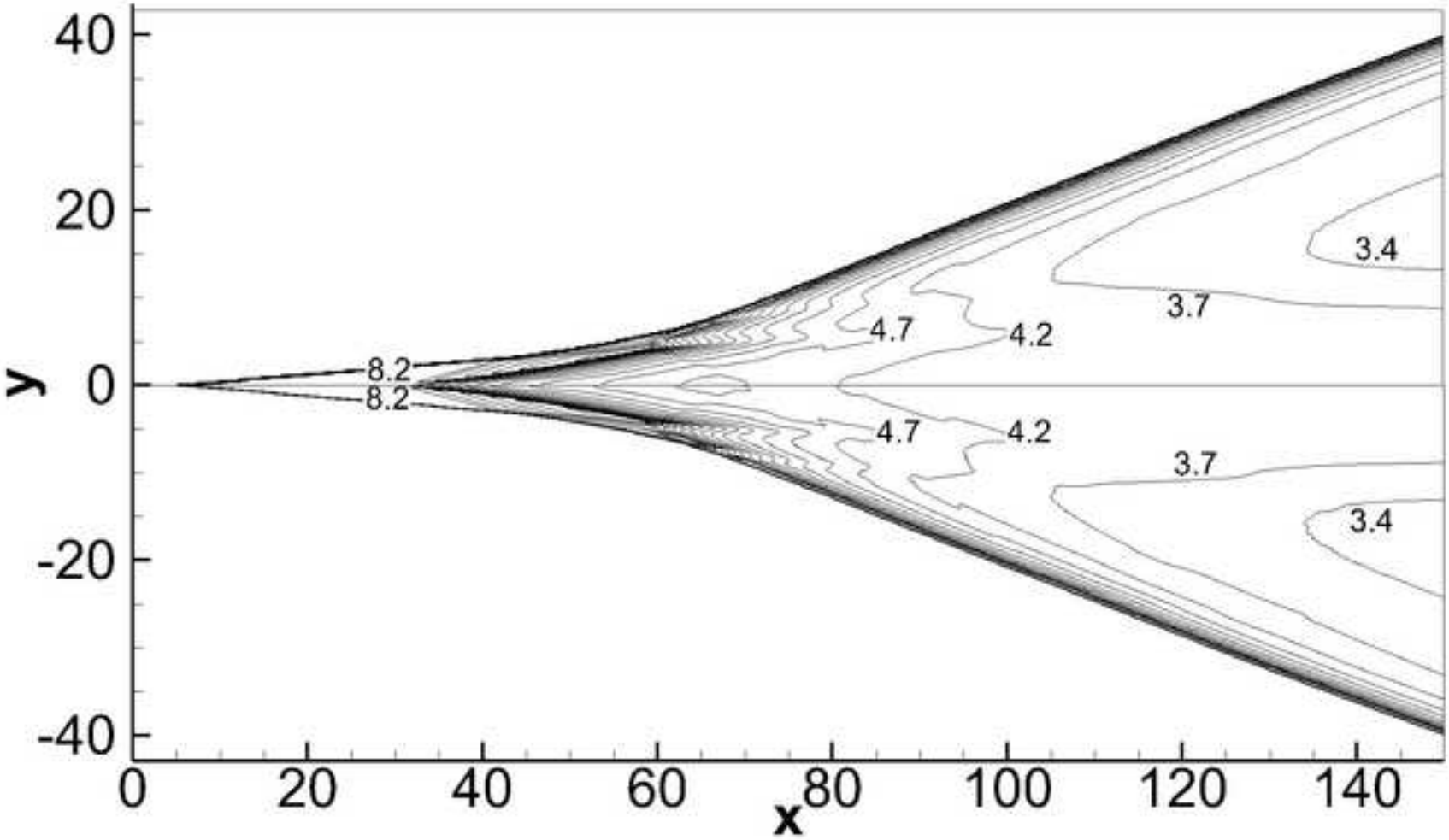

Figure 3
Click here to download high resolution image

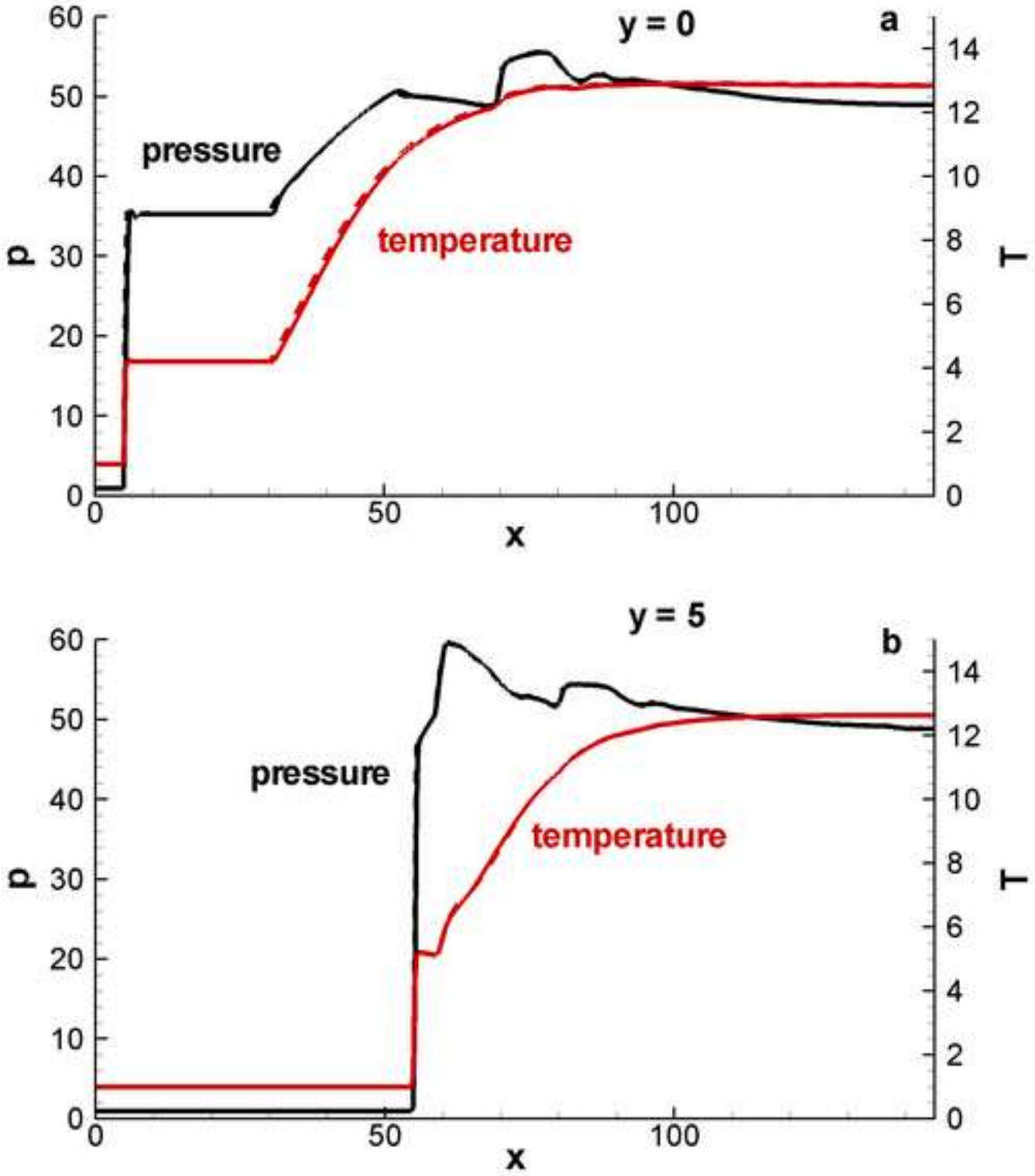

Figure 4

Click here to download high resolution image

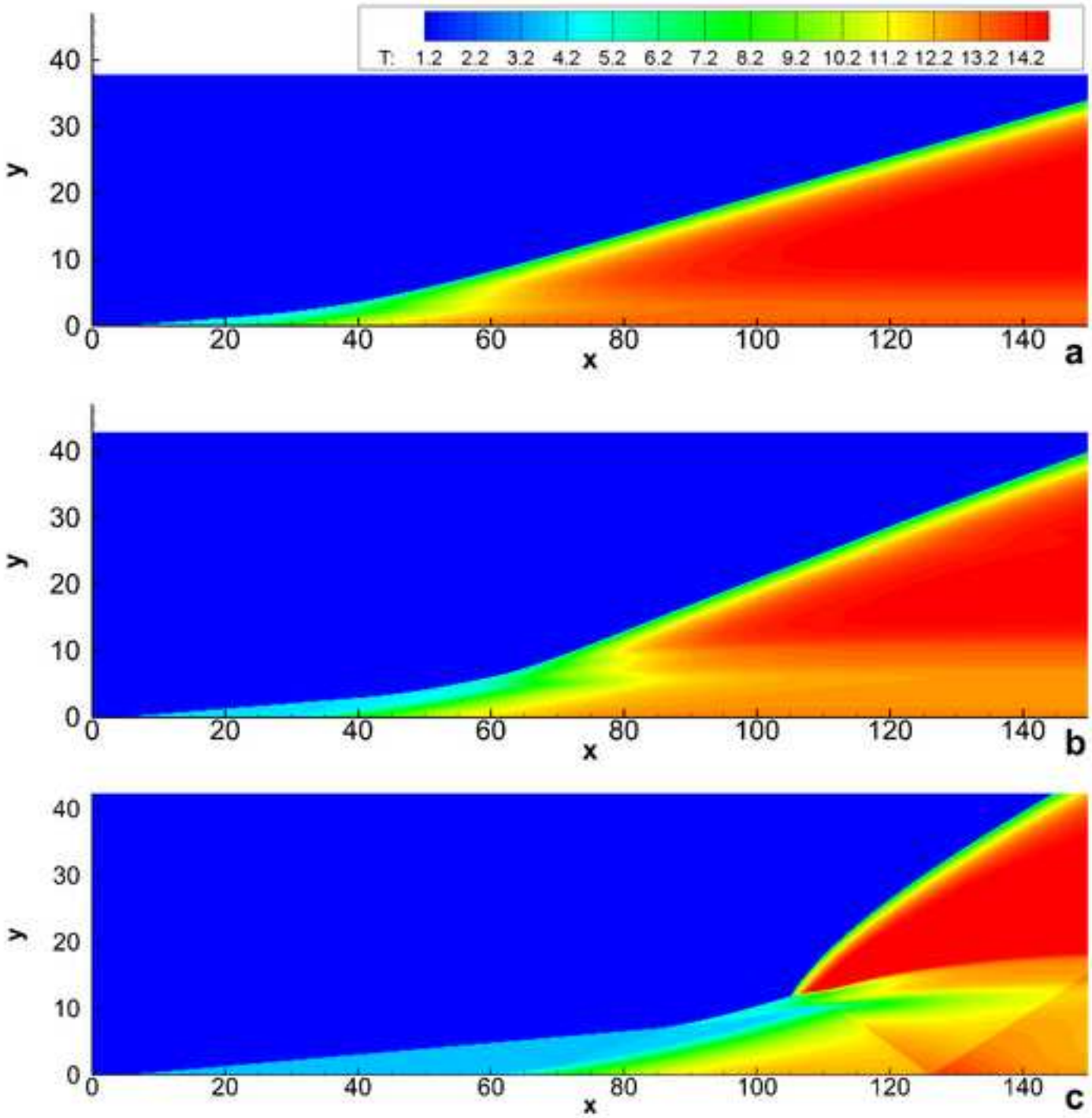

Figure 5
Click here to download high resolution image

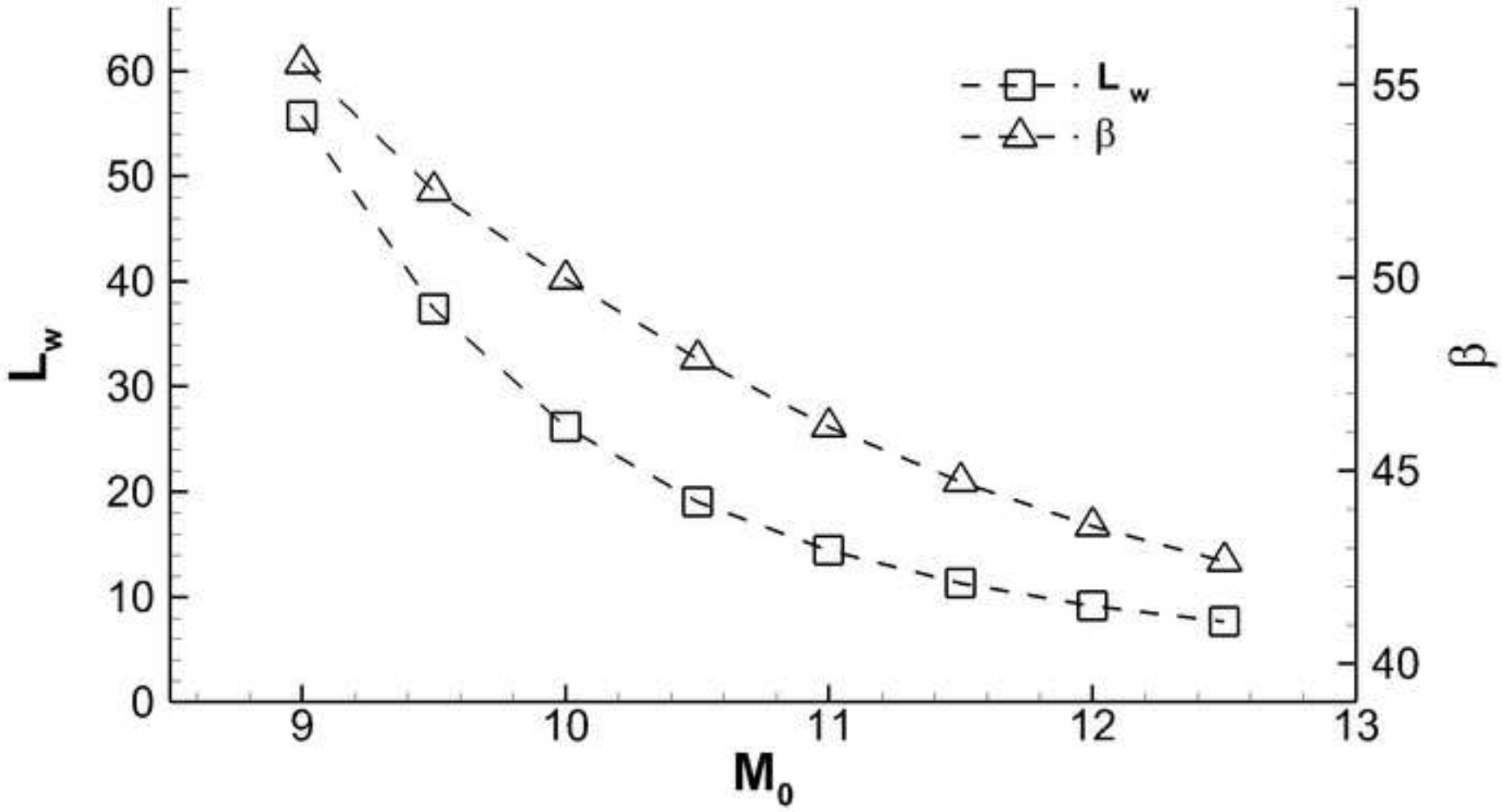

Figure 6
Click here to download high resolution image

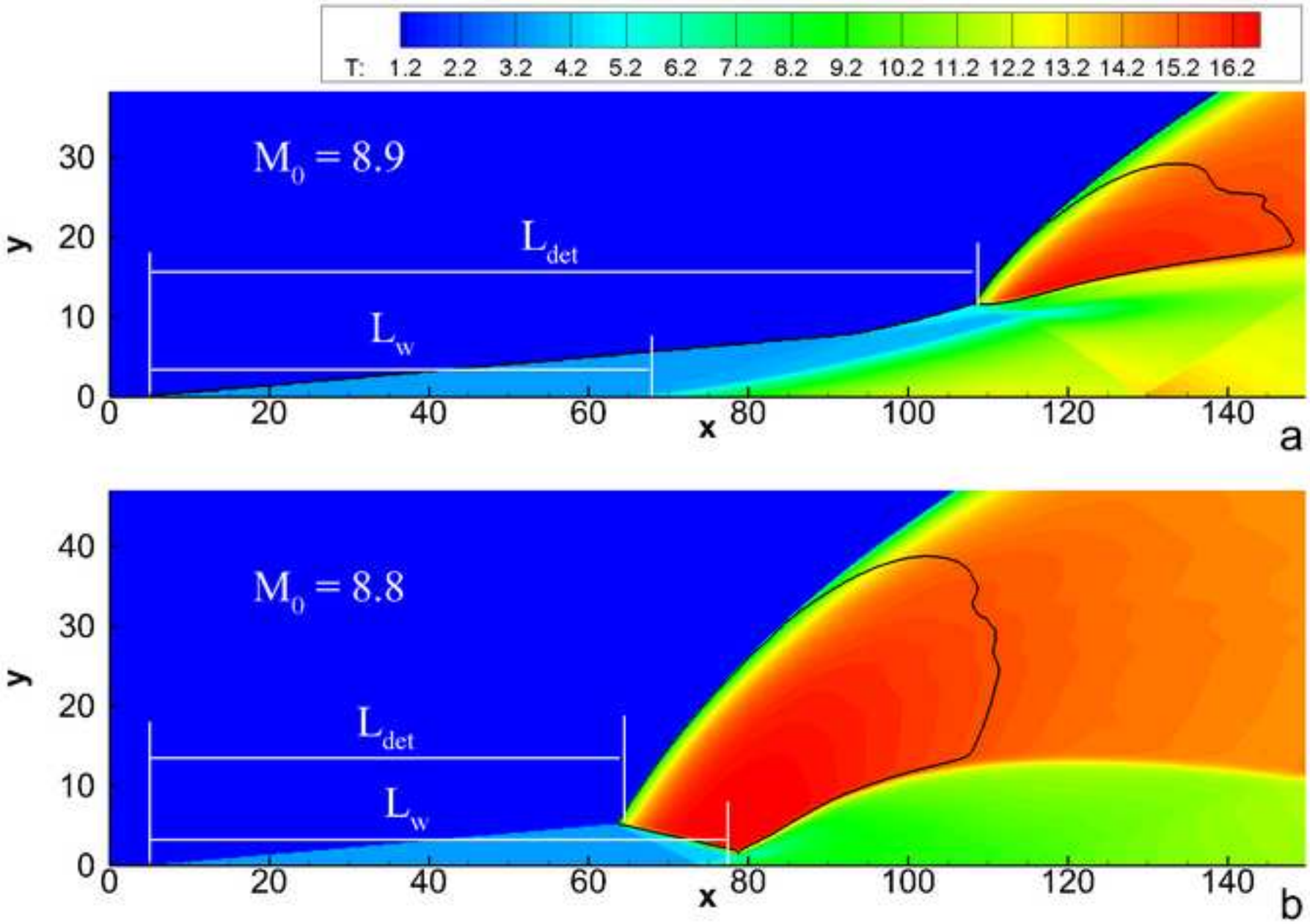

Figure 7
Click here to download high resolution image

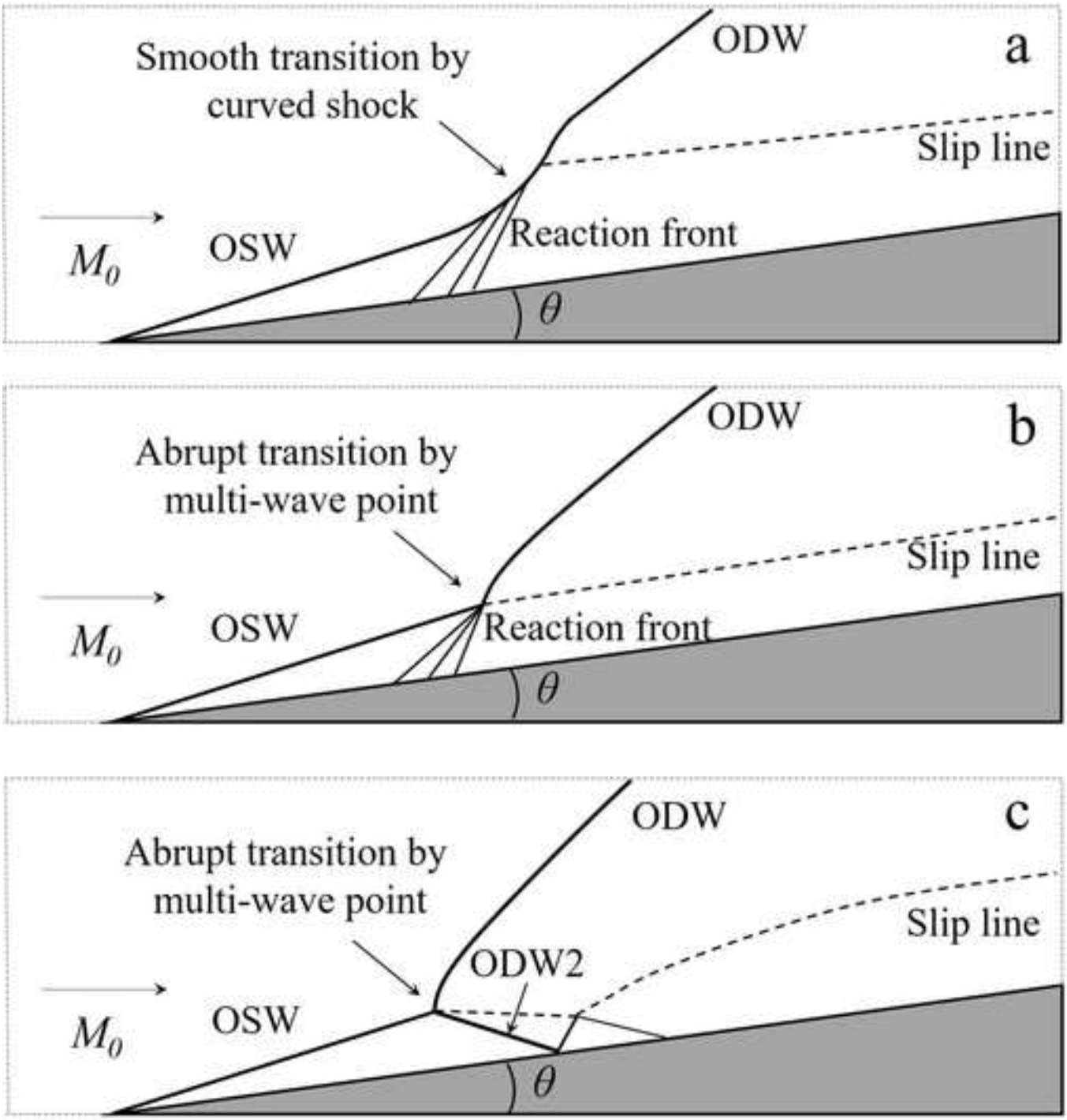

Figure 8
Click here to download high resolution image

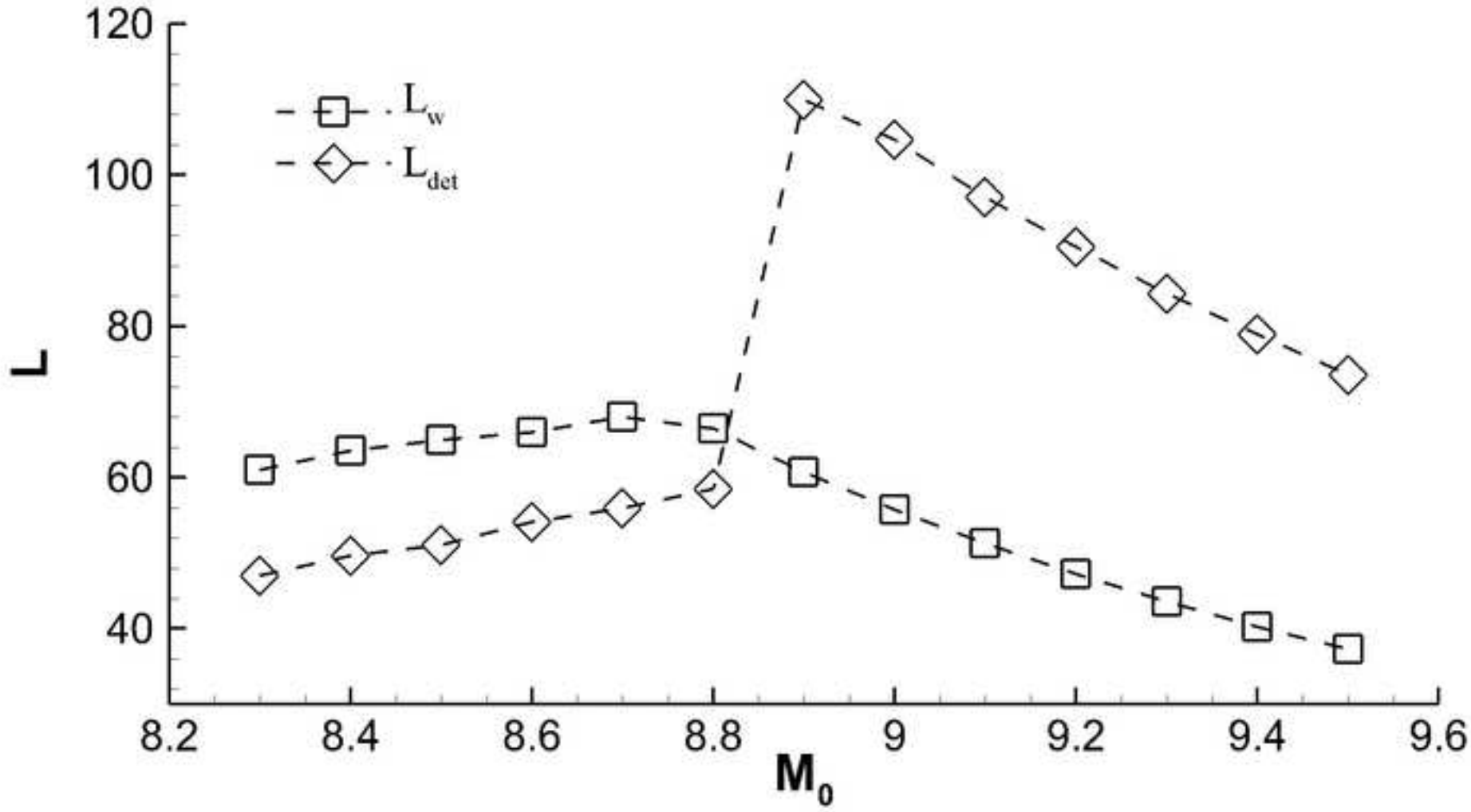

Figure 9
Click here to download high resolution image

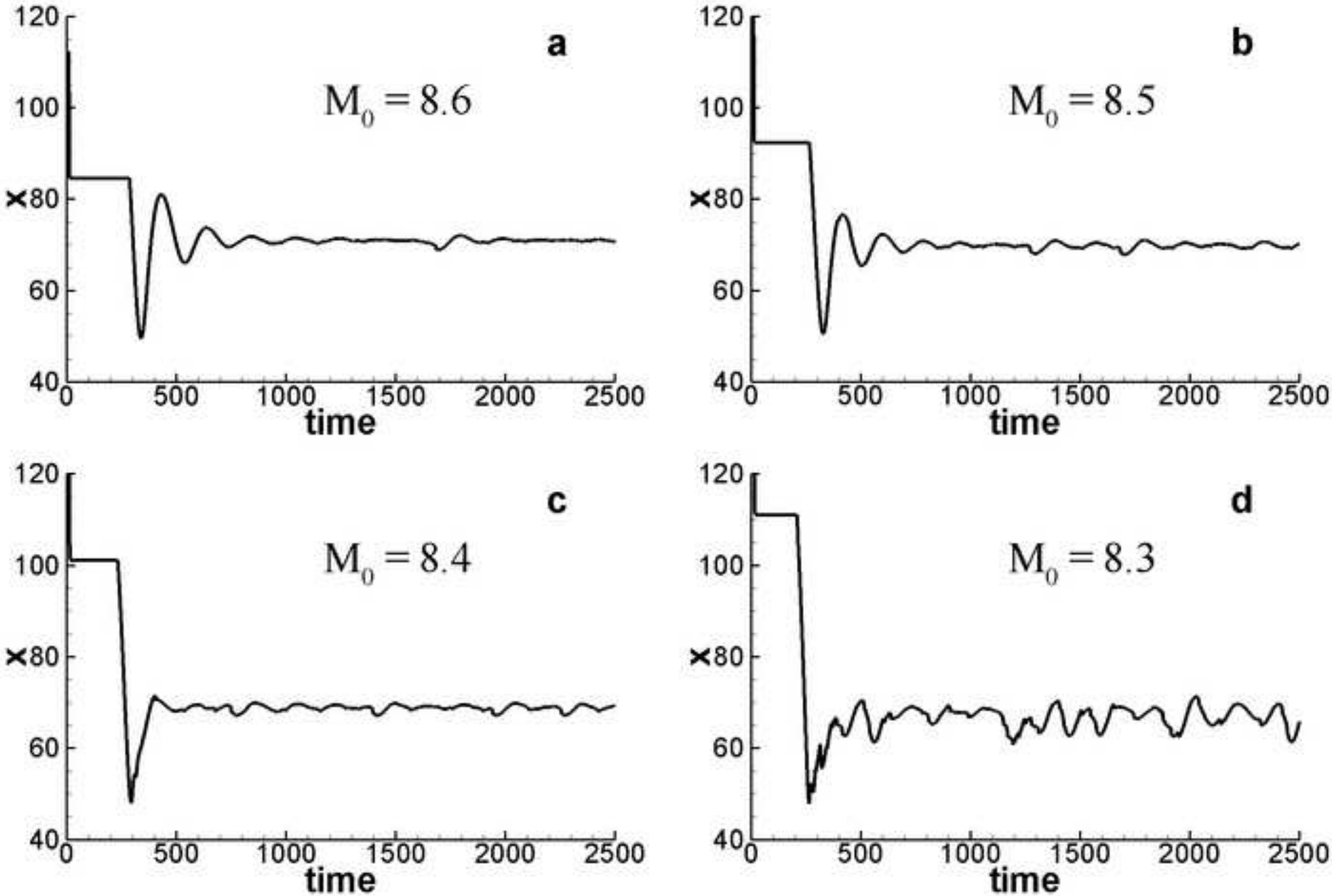

Figure 10
Click here to download high resolution image

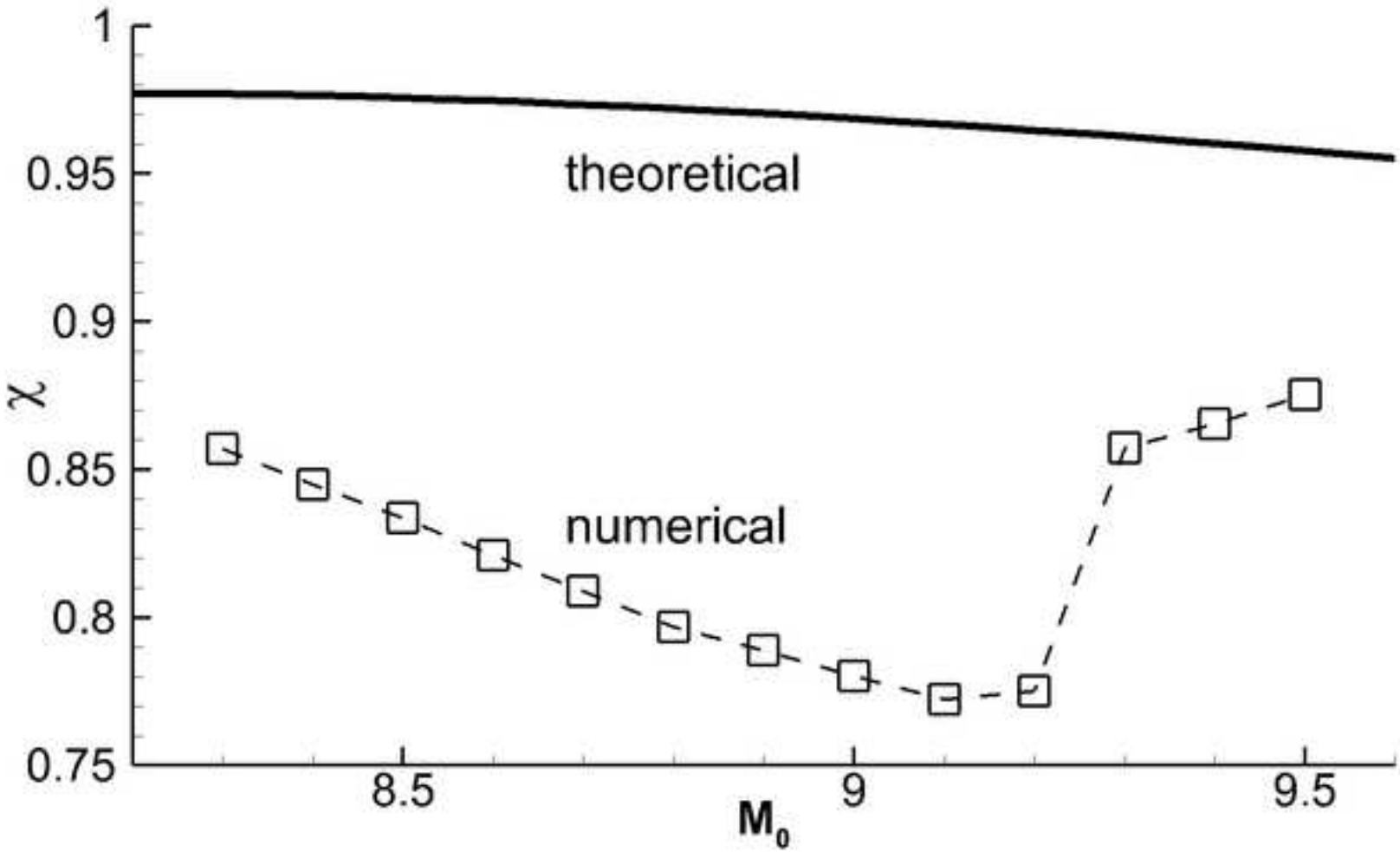

Figure 11
Click here to download high resolution image

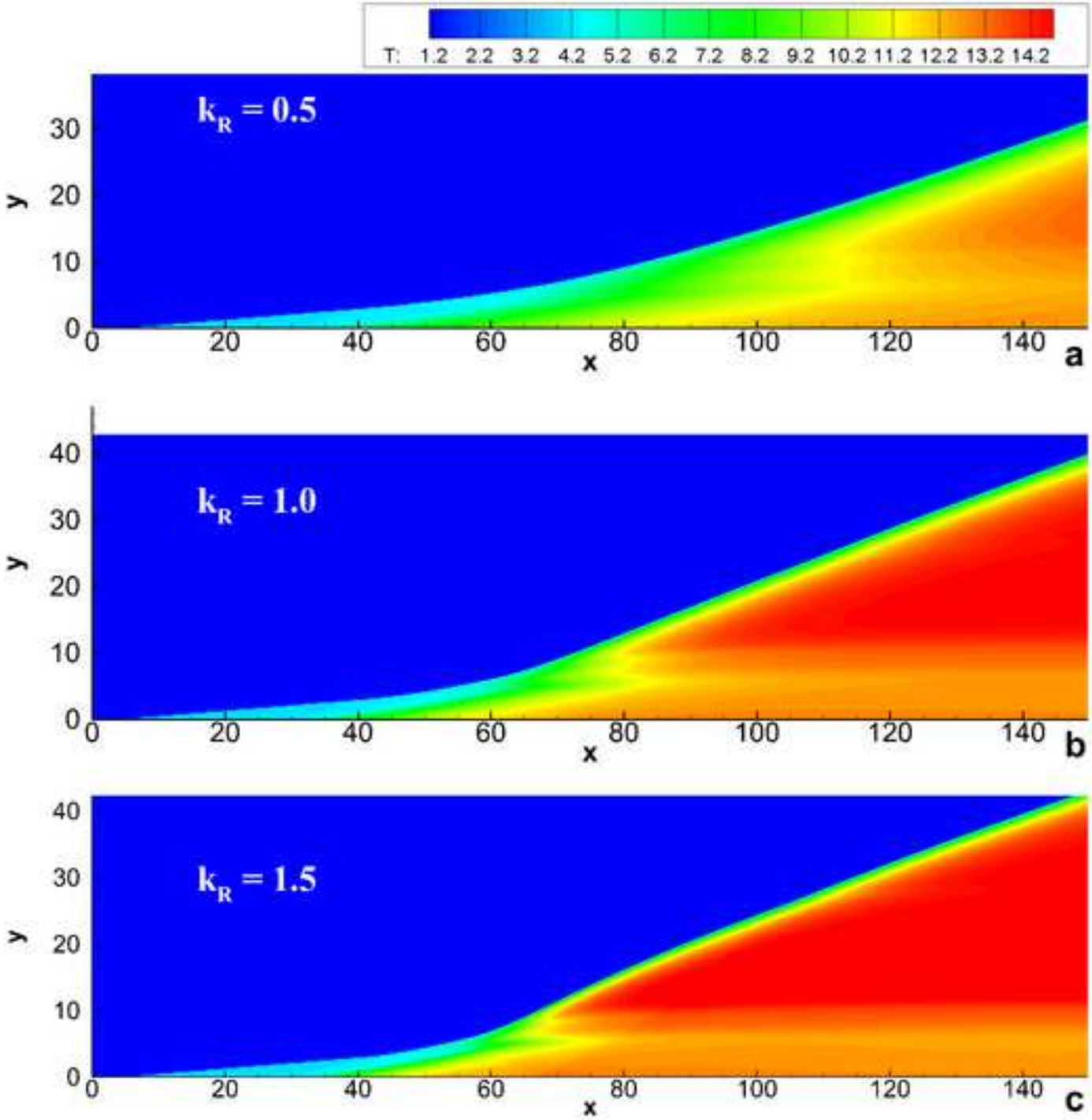

Figure 12
Click here to download high resolution image

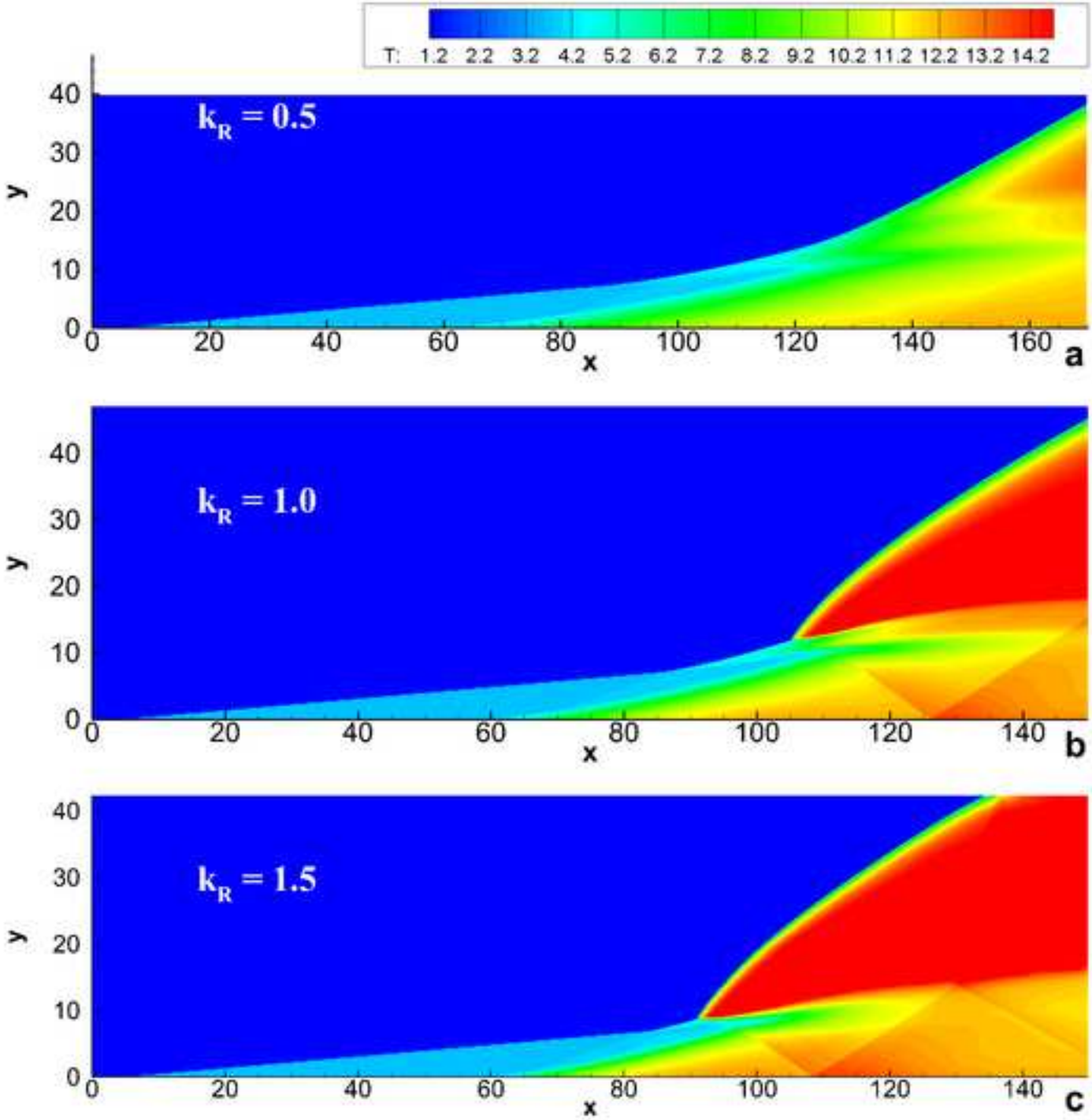

Figure 13
Click here to download high resolution image

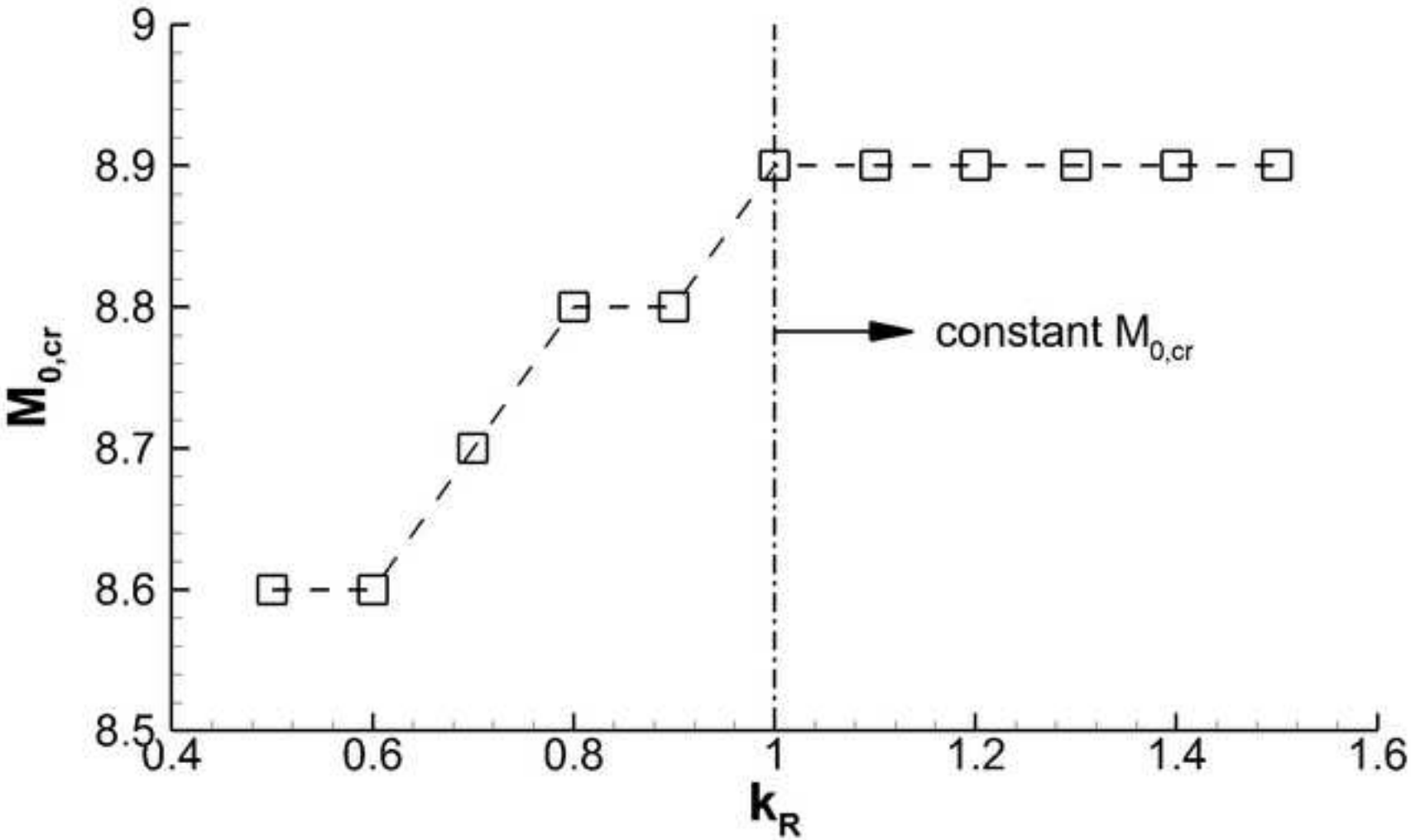

Figure 14
Click here to download high resolution image

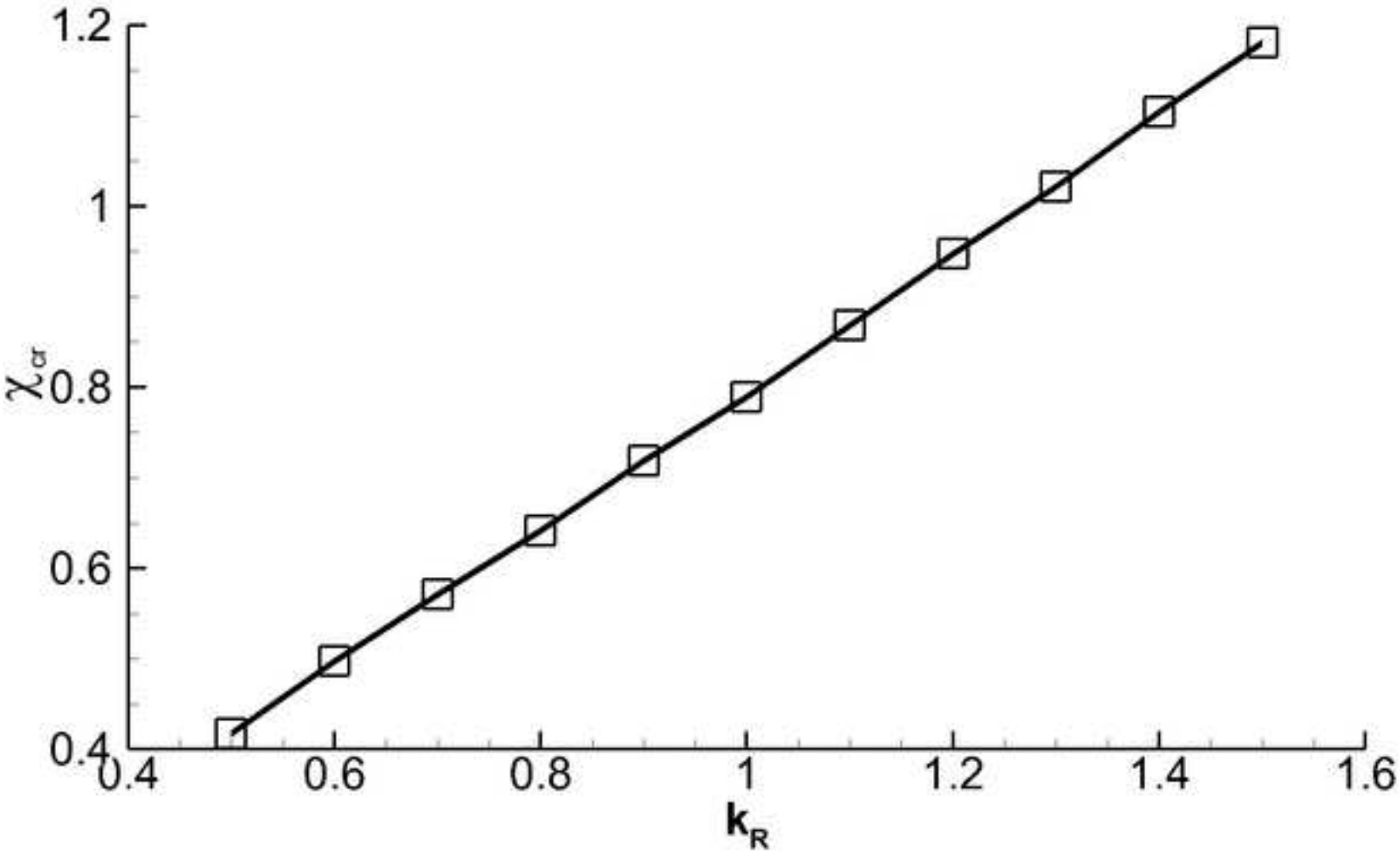

Appendix Figure b1

Click here to download high resolution image

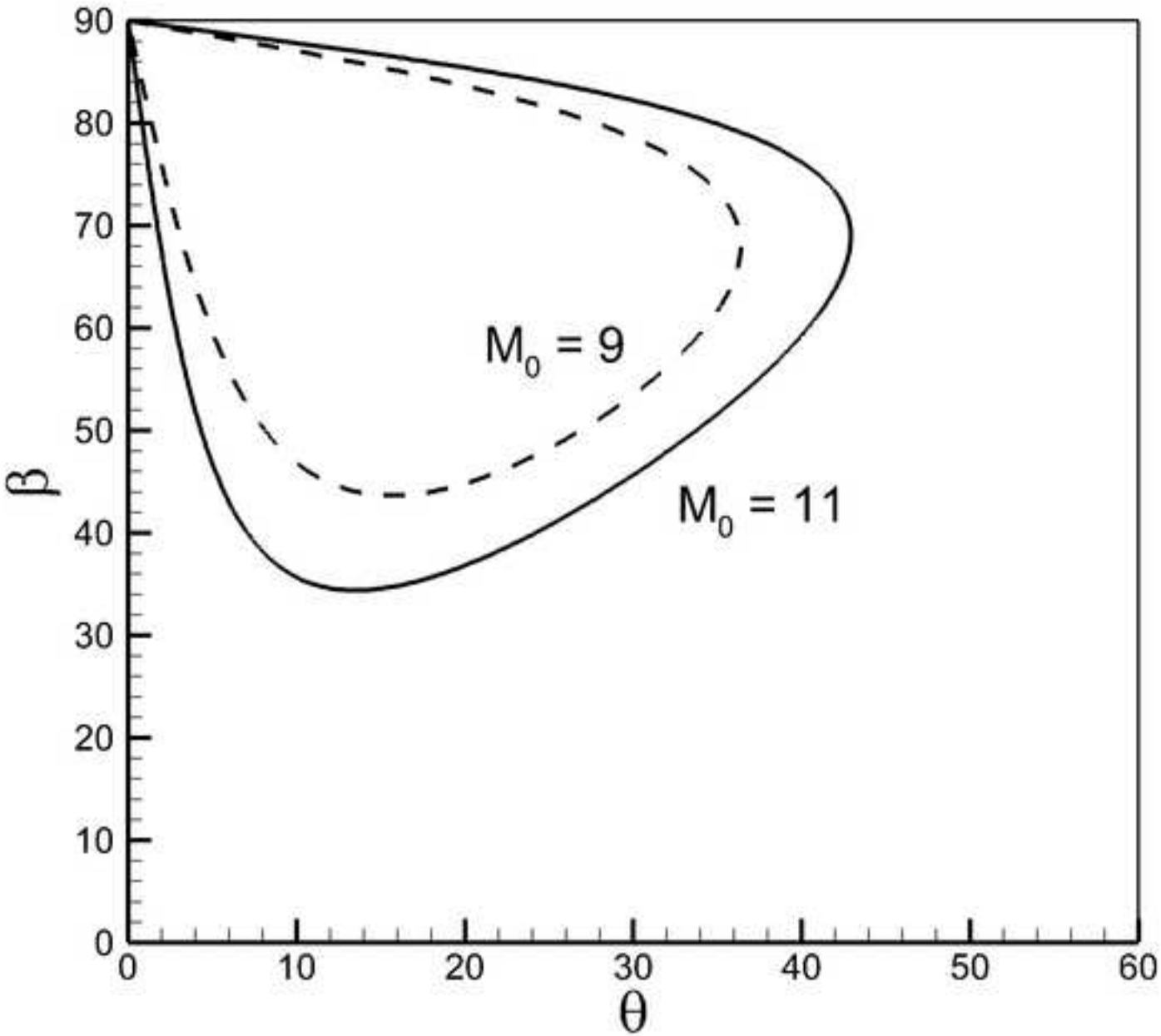

Appendix Figure b2

Click here to download high resolution image